Available online at www.sciencedirect.com
ScienceDirect
Journal of Sound and Vibration 312 (2008) 672–693
JOURNAL OF SOUND AND VIBRATION
www.elsevier.com/locate/jsvi

Multisensor approaches for chatter detection in milling

E. Kuljanic, M. Sortino*, G. Totis

DIEGM– Department of Electrical, Managerial and Mechanical Engineering, University of Udine, Via delle Scienze, 208, I-33100 Udine, Italy

Received 24 July 2007; received in revised form 5 November 2007; accepted 6 November 2007
Available online 20 February 2008

Abstract

The development of a chatter detection system for application in industrial conditions was investigated. Several sensors—rotating dynamometer, accelerometers, acoustic emission and electrical power sensors—were compared to determine which signals are most sensitive to chatter onset. The signal characteristics both in time and frequency domain were condensed into a set of chatter indicators, which were further elaborated by means of statistical basic concepts, in order to obtain a chatter identification system. Single-sensor systems and multisensor systems were compared both in terms of accuracy and robustness against malfunctions. Among single sensor systems, the cutting torque signal proved to be a superior signal for chatter identification. Multisensors systems composed of three or four sensors are the most promising solution for reliable and robust chatter identification. The best results were obtained by the multisensor system composed of the axial force sensor and accelerometers.

1. Introduction

In recent years, the competitiveness of international markets is increasing the interest in unmanned machining systems or intelligent machining systems, where most of the productive activities are performed without the operator.

In the new conditions, the machine tool should be able to perform automatically several activities, such as: detection and suppression of vibrations and chatter, tool condition monitoring, optimization of cutting parameters, collision detection and prevention and others.

Chatter is a vibrational phenomenon which arises in machining processes for specific combinations of cutting parameters. It is a very complex phenomenon characterized by unstable, chaotic motions of the tool and by strong anomalous fluctuations of cutting forces. The onset of chatter may cause abnormal tool wear or tool breakage, damage of both the tooling structure and the spindle bearings, poor surface roughness and poor dimensional accuracy of the workpiece. In the last decades, many researchers have focused on the development of analytical and numerical methods for the prediction of chatter [1,2]. However, these methods are difficult to apply for chatter prevention in industrial conditions since a good estimation of the machining system dynamics and cutting forces is required.

*Corresponding author. Tel.: +39 432 558241; fax: +39 43 2558251.
E-mail address: sortino@uniud.it (M. Sortino).

0022-460X/$ - see front matter © 2007 Elsevier Ltd. All rights reserved.
doi:10.1016/j.jsv.2007.11.006

An automatic system for chatter detection and suppression is an alternative solution to this problem. There are several methodologies that can be applied effectively for the suppression of chatter, for instance: mechanical dampers, actuators, spindle speed regulation or modulation systems [2,3]. The spindle speed regulation system is the most practical approach for chatter suppression since it does not require any modification of the machine tool or tool holder. For instance, as soon as the chatter onset is identified by an adequate chatter identification system, the control system can automatically vary the cutting speed until a stable condition is reached, as proposed by Liao et al. [4] and by Tarng et al. [5]. However, there is a need for a reliable method for automatic detection of chatter in industrial conditions.

The characteristics of the identification system are similar to those proposed by Tarng [6] in 1988 for tool breakage detection systems, as follows: reliability, robustness, responsiveness, flexibility and practicality. In addition, the application in industrial conditions implies the following requirements:

1. it should not modify the modal parameters of the machining system, in particular it should not reduce the stiffness of the machine tool;
2. it should be compatible to pallet changer and to tool changer;
3. it should not put constraints on the selection of cutting parameters and on any other machining condition (tool dimensions, workpiece dimensions, tool geometry, and others);
4. the functioning of the chatter detection system should not rely on the knowledge of the actual cutting conditions and on a priori knowledge of the machining system dynamics;
5. the system should be insensitive to environmental noise.

In this work, the application of several different types of sensors—rotating dynamometer, accelerometers, acoustic emission sensor and electrical power sensor—and the methodologies for chatter detection in face milling are discussed and tested with experimental data, in order to determine which sensor type or which combination of sensors is more suitable for industrial application.

2. Chatter identification systems

In recent years, many researchers have investigated the application of sensors for chatter detection in machining operations.

Table 1 illustrates some research works focused on chatter identification systems. The table is organized to indicate the machining process considered in the research, the sensor or sensors used, the applied signal processing techniques or classification methods and the authors' reference.

Several contributions have investigated chatter identification systems in milling. The sensors which are mostly applied are the plate dynamometer, the microphones, the displacement and acceleration sensors.

In relation to the signal processing and classification methods, the methods of analysis in the frequency domain (power spectral density—PSD, fast fourier transform—FFT and wavelet transform—WT) are the most common. All these classification methods are based on the analysis of the energy distribution in the signal spectrum.

The analysis of the signal in the time domain was also commonly applied by using the once per revolution sampling—OPRS. This method is based on the analysis of the signal values sampled once per spindle revolution and the dispersion of data is used to determine the onset of chatter. From the publications it can be seen that the vibrations of the tool tip measured by applying displacement probes—for instance, eddy current or laser–can be used to identify the chatter in milling.

The application of a microphone for chatter detection purposes in milling has been investigated by several authors. According to Delio et al. [7], microphone is very suitable for chatter detection in milling, being its sensitivity to chatter onset comparable to that of other sensors such as plate dynamometers, displacement probes and accelerometers. Nevertheless, microphones are affected by some limitations such as directional considerations, low-frequency response, and environmental sensitivity. Particularly, the suppression of environmental noise is mandatory for a successful application of microphones.

For chatter identification, both the frequency bandwidth of the sensor and its location are crucial. Specifically, the frequency bandwidth of the sensor must be sufficient to detect the possible frequency range of

Table 1
Summary of chatter identification systems research

Process	Sensors	Signal processing and classification methodology	Reference
Milling	Microphone	PSD	[7]
Turning	Accelerometers	Cross coherence of accelerations in two directions	[8]
Milling	Eddy current displacement sensors and plate dynamometer	PSD and qualitative analysis of time trajectories	[9]
Milling	Laser displacement sensor	Qualitative analysis of tool vibration in time	[10]
Turning	Plate dynamometer under the turret	Entropy rate of the signal	[11]
Turning	Plate dynamometer under the turret	Time series analysis of the force signals	[12]
Milling	Microphone	Variance of OPRS	[13]
Milling	Plate dynamometer	WT	[14]
Milling	Eddy current displacement sensors	OPRS, PS, PSD of tool trajectory (quantitative chatter indicators not specified)	[15]
Milling	Plate dynamometer and Microphone (harmonizer)	PSD	[16]
Milling	Plate dynamometer	FFT	[17]
Milling	Laser displacement sensor	OPRS, PS, PSD of tool trajectory (quantitative chatter indicators not specified)	[1]
Milling	Microphone	PSD	[18]

OPRS = Once per revolution sampling; PS = Poincaré sections; PSD = power spectral density; FFT = fast Fourier transform; WT = Wavelet transform.

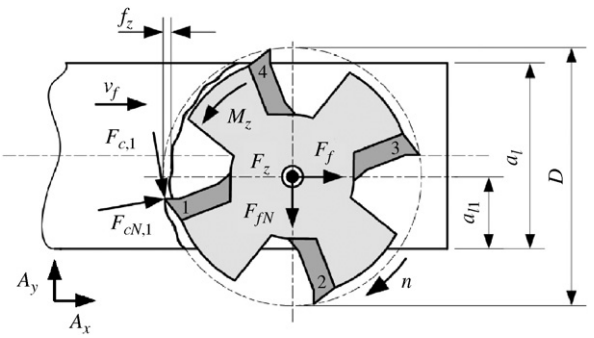

Fig. 1. Face milling geometry.

chatter vibrations, typically from 100 to 5000 Hz. The general rule for sensor location is that the closer the sensor to the source, the more reliable are its measurements [7].

3. Design of experiments and experimental procedures

In order to investigate the application of sensors for detection of chatter in milling, several tests in face milling were performed. The general set up of the face milling tests is in Figs. 1 and 2. Two tests configurations had been used, as given in Table 2.

For each test configuration, the frequency response of the system and the first natural frequency were estimated by applying the pulse test method [19]. In both configurations, the extension was included in the tooling structure in order to reduce the stiffness of the system (Fig. 2).

Three designs of experiments—DOE were performed (Table 3). The number of tests for DOE number 1 was 36, whereas it was 12 for both DOE number 2 and 3. In each test, the depth of cut was increased by discrete increments of 0.1 mm from 0.4 mm until severe chatter occurred. The test was stopped at a depth of cut of 1.8 mm if no chatter was observed.

The total number of experimental points was 287; 191 stable points and 96 unstable points.

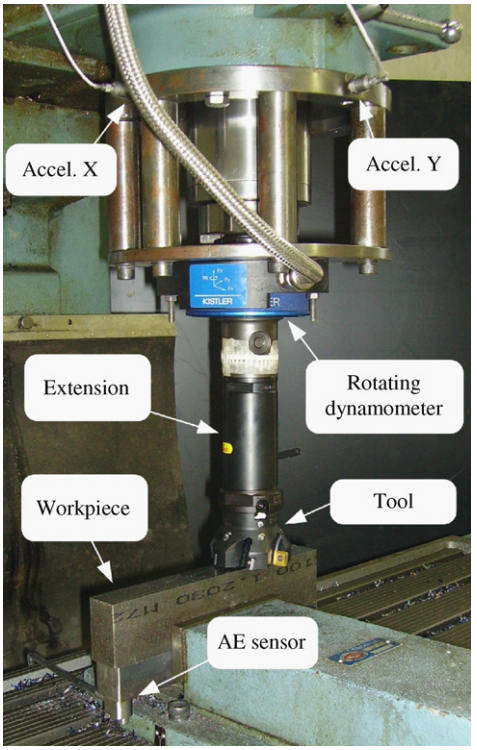

Fig. 2. Experimental setup.

Table 2
Face milling cutters

Config	Cutter (mill)	Res. Freq. (Hz)
1	Stellram face milling cutter, diameter $D = 50$ mm, tool cutting edge angle $\chi = 90°$, number of teeth $z = 5$, inserts APKT1604PDER-43 SP6564, facet	274
2	Sandvik- Coromant face milling cutter, diameter $D = 80$ mm, tool cutting edge angle $\chi = 90°$, number of teeth $z = 6$, carbide inserts R290-12 T3 08M-PM P4040, nose radius $r_\varepsilon = 0.8$ mm, wiper dimension $b_s = 1.53$ mm,	189

Table 3
Design of experiments

DOE	Conf.	Width of the workpiece and cutter position	Factors	Levels	Nominal values	N.o.t.
1	1	$a_L = 30$ mm	n	6	860, 1100, 1400, 1870, 2370, 3000 (rpm)	36
			f_z	2	0.07 and 0.12 (mm)	
			a_{LI}	3	7, 15, 23 (mm)	
2	1	$a_L = 48$ mm	n	6	860, 1100, 1400, 1870, 2370, 3000 (rpm)	12
		$a_{LI} = 23$ mm	f_z	2	0.07 and 0.12 (mm)	
3	2	$a_L = 30$ mm	n	6	510, 640, 860, 1100, 1400 (rpm)	12
		$a_{LI} = 30$ mm	f_z	2	0.07 and 0.12 (mm)	

N.o.t. = Number of tests.

Tests were performed on a Rambaudi M3P milling machine with one tooth in the cutter and dry milling. The results obtained with this configuration can be extended without changes to configurations where multiple tooth cutters are applied and run-out is present. The workpiece material was Ck45, Brinell hardness 191 HB, $30 \times 80 \times 250\,\text{mm}^3$, clamped on a vice.

The main cutting force F_c, cutting perpendicular force F_{cN}, axial cutting force F_z and torque M_z were measured by using a Kistler 9123C rotating dynamometer clamped between the cutter and the spindle (Fig. 2). The feed force F_f and the feed perpendicular force F_{fN} were calculated by rotation of the cutting force F_c and of cutting perpendicular force F_{cN} components. Accelerations in the X and Y directions A_X and A_Y (see Fig. 1), were detected by Kistler accelerometers type 8704B50 mounted on the spindle housing. The electrical power absorbed by the main spindle motor P_{el} was measured by a Prometec EPT20 electrical power sensor. The acoustic emission root mean square signal AE_{rms} was measured by Kistler acoustic emission sensor type 8192B (50–400kHz frequency range, integrating time constant 0.12 ms) clamped on the vice.

All sensor signals were sampled at a frequency of 20 kHz by using a National Instruments data acquisition board and stored for later analysis. The working environment for data elaboration and analysis was Mathworks Matlab.

4. Analysis of data

The analysis of data was performed in two steps. First, preliminary analysis was carried out in order to determine the characteristics of the sensor signals, then the chatter indicators were designed and their characteristics were compared.

4.1. Preliminary analysis

4.1.1. Rotating dynamometer

The characteristic and spectra of the cutting forces measured by the rotating dynamometer both in stable and unstable conditions are in Figs. 3–7.

The analysis in the time domain of cutting forces evidenced that the signal is periodic and stationary when the system is stable, whereas some anomalies were present when the system was unstable. For instance, the amplitude of fluctuations is not constant in Fig. 4c and there are some torque peaks in Fig. 7c.

The analysis of the cutting forces signals in stable conditions and in the frequency domain confirmed that the peaks of the spectra are located at the integer multiples of the spindle revolution frequency—SRF, Figs. 3b, 4b, 6b, 7b).

In the Figures, the SRF frequencies were first calculated and the SRF peaks were evidenced by using squares. All other peaks, or anomalous peaks, were identified and denoted by circles.

Anomalous peaks, or "chatter peaks", were dominant in unstable conditions (Figs. 3d, 4d, 6d and 7d). This is in accordance to Insperger et al. [20]. It was also noticed that the maximum chatter peaks are located at the resonance frequency of the tool–tool holder–dynamometer–spindle mechanical system, (Figs. 3d and 4d).

The feed force F_f and the feed perpendicular force F_{fN} measured by the rotating dynamometer are proportional to the displacements of the cutter u_f and u_{fN}, respectively. Therefore, a good estimate of cutter vibrations can be obtained by analysis of these cutting force components.

Analysis of the trajectory of the system in the working plane (F_f, F_{fN}) and of the once per revolution samples is given in Fig. 5. The trajectory is periodic in cases $a_p = 0.5$ mm and $a_p = 0.8$ mm and the dispersion of OPRS is low; in the case $a_p = 1.0$ mm the system is becoming unstable and the OPRS are more scattered; the trajectory is aperiodic and chaotic and the OPRS are spread for $a_p = 1.1$ mm.

The characteristic of the axial force F_z component is very noisy since the system is very stiff in the axial direction and the sensitivity of the dynamometer is limited (Fig. 6).

The cutting torque M_z is highly influenced by chatter since it is proportional to the uncut chip thickness which is perturbed by the regenerative effect (Fig. 7).

It is difficult to apply the rotating dynamometer in industrial conditions since it is not compatible to tool changer, it reduces the stiffness of the system and it limits the selection of cutting parameters. Moreover, according to Delio et al. [7], the main limit for the application of dynamometers for chatter detection in milling is their limited bandwidth, which is less than 1 kHz. Therefore, dynamometers can be applied successfully in face milling, whereas they may be inadequate for application in end milling and finishing.

Since the resonance frequencies of the test configurations proposed in this work were rather low (Table 2), the rotating dynamometer was suitable for chatter detection.

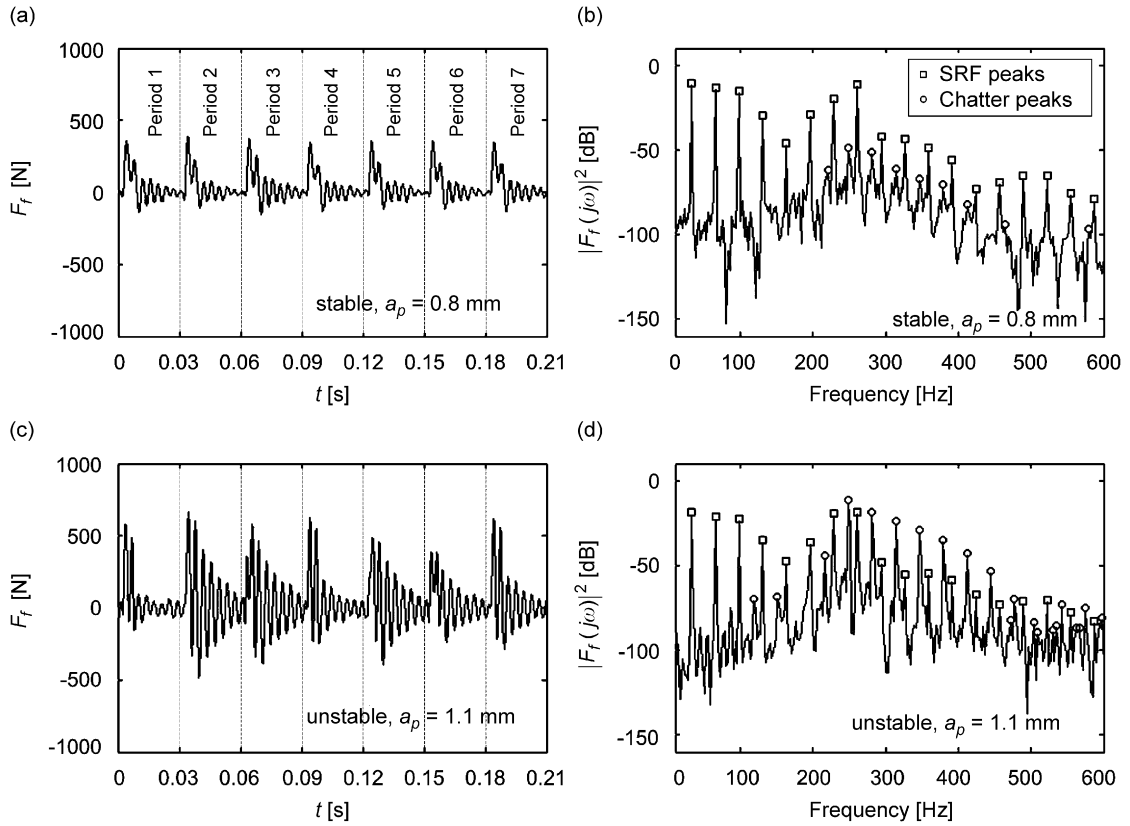

Fig. 3. Characteristics in time and spectra of the feed force F_f both in stable (a) and (b), and unstable conditions (c) and (d). Cutter configuration 1, $a_L = 30$ mm, $a_{L1} = 23$ mm, $n = 1870$ rev/min, $f_z = 0.07$ mm.

Also, it has to be pointed out that the bandwidths of the axial force F_z and torque component M_z were significantly higher than those of the other force components.

In addition, these components can be measured by using sensors with better frequency responses and less invasive than the rotating dynamometer, such as force rings, active bearings, and others [21]. Therefore, chatter identification systems based on these components can be successfully applied in a wider range of applications than face milling.

4.1.2. Accelerometers

The characteristic and spectra of the accelerations measured by the accelerometers are given in Figs. 8 and 9.

The behaviour of the acceleration signals is similar to cutting force signals: the signals are periodic in stable conditions while anomalies emerge in unstable conditions. For example, the behaviour of signal A_X and the amplitude of signal A_Y change abruptly when a_p is 1.1 mm (Figs. 8c and 9c). Also, there is a proliferation of additional frequencies in unstable conditions (Figs. 8d and 9d).

The trajectories and the OPRS of the (A_X,A_Y) vector are shown in Fig. 10. The trajectory is periodic in cases $a_p = 0.5$, 0.8 and 1.0 mm; the trajectory is aperiodic and chaotic for $a_p = 1.1$ mm. The dispersion of OPRS is low when depth of cut a_p is between 0.5 and 1.0 mm whereas it is high in Fig. 10d. The increase in unstable conditions of variance of the accelerations signals OPRS is smaller than that of the cutting force signals in the working plane. Also, its sensitivity to chatter is strongly influenced by the point of the trajectory taken as a reference.

In comparison to the cutting forces measured by the dynamometer, the acceleration signals have wider spectra (about 5 kHz) than the cutting force signals (less than 1 kHz); therefore, they are suitable for a wider

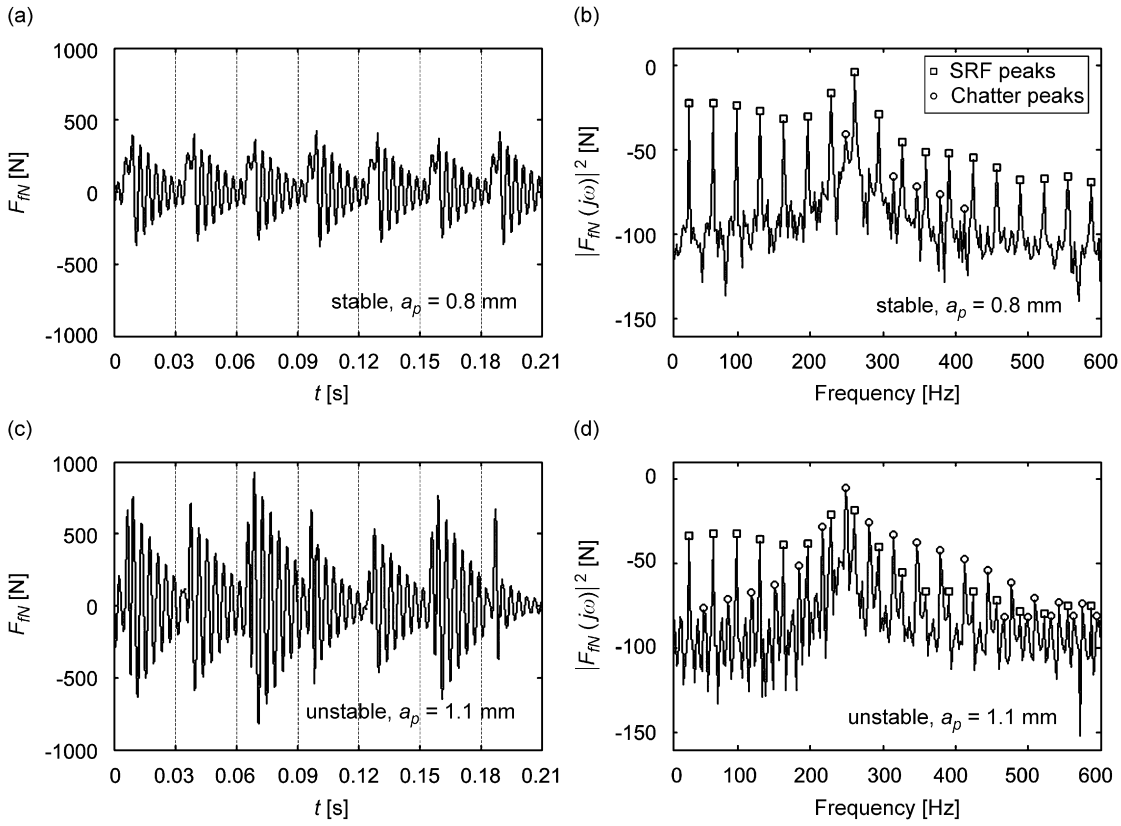

Fig. 4. Characteristics in time and spectra of the feed perpendicular force F_{fN} both in stable (a) and (b), and unstable conditions (c) and (d). Cutter configuration 1, $a_L = 30$ mm, $a_{LI} = 23$ mm, $n = 1870$ rev/min, $f_z = 0.07$ mm.

range of applications. However, according to Delio et al. [7], the placement of the sensor is a difficult task since it requires prior knowledge of the dynamic behaviour of the machine tool.

4.1.3. Acoustic emission and electrical power

The acoustic emission signal AE_{rms} is periodic in the time domain, and there are irregular peaks when the tooth enters or leaves the workpiece (Fig. 11a and c). There are not relevant changes in the characteristic when the machining system becomes unstable.

The chatter peaks of the AE_{rms} spectra are present both in stable and unstable conditions (Fig. 11b and d). Therefore, the identification of chatter by using the AE_{rms} signal is more difficult than by using the acceleration or force signals.

The characteristic of the main spindle electrical power P_{el} is not periodic and not related to the machining dynamics (Fig. 12a and c).

The frequency content of P_{el} spectra is poor and it is limited to the lowest frequencies (less than 100 Hz). No peaks related to SRF or chatter are visible both in stable and unstable conditions Fig. 12b and d).

The analysis of the electrical power signal P_{el} both in time and frequency domain evidenced that this sensor may be applied only in cases where the SRF is very low.

4.2. Chatter indicators

According to the signals characteristics discussed in the previous sections, chatter indicators were designed in order to vary in the range from 0—system stable to 1—system extremely unstable.

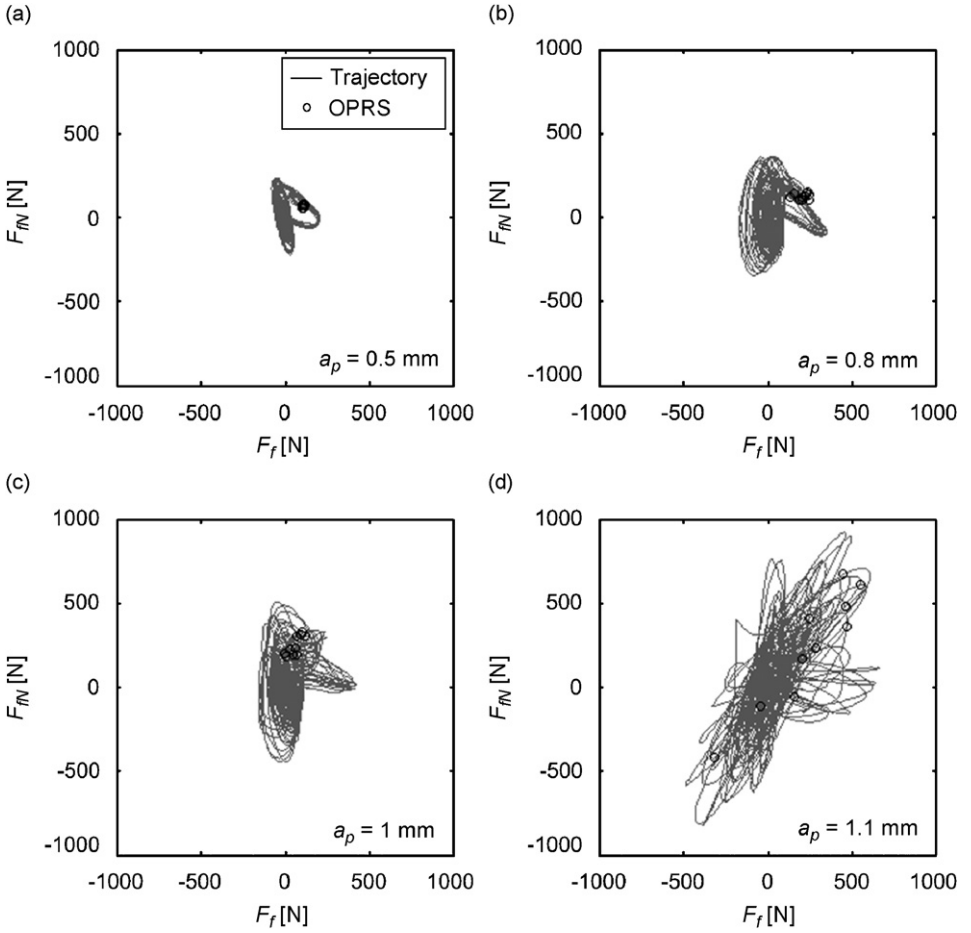

Fig. 5. Analysis of the trajectory of the system and OPRS in the F_f and F_{fN} plane. Cutter configuration 1, $a_L = 30$ mm, $a_{LI} = 23$ mm, $n = 1870$ rev/min, $f_z = 0.07$ mm.

A good estimate of the actual spindle speed is required to calculate the chatter indicators, which may be obtained from the numeric control of the machine tool or by simple analysis of the cutting force, acceleration or acoustic emission signals.

4.2.1. Time-domain chatter indicators

The onset of aperiodic components in the signals is the main effect of chatter in the time domain. Every sensor signal $S(t)$ can be expressed as the sum

$$S(t) = S_p(t) + S_a(t), \tag{1}$$

where $S_p(t)$ is the τ-periodic component and $S_a(t)$ is the aperiodic component, being τ the spindle revolution period. It has to be pointed out that the reference period is τ also for cutters with multiple teeth due to the run-out.

The periodic component contains the harmonics of the SRF, while all other components are included in the aperiodic term.

The auto-correlation coefficient ρ_S^2 was used to determine the strength of the periodic component in the signal as follows:

$$\rho_S^2 = \frac{1}{\tau \cdot \sigma_S^2} \int_{t-\tau}^{t} S(\theta) S(\theta - \tau) \mathrm{d}\,\theta, \tag{2}$$

where σ_S is the standard deviation of the signal in time.

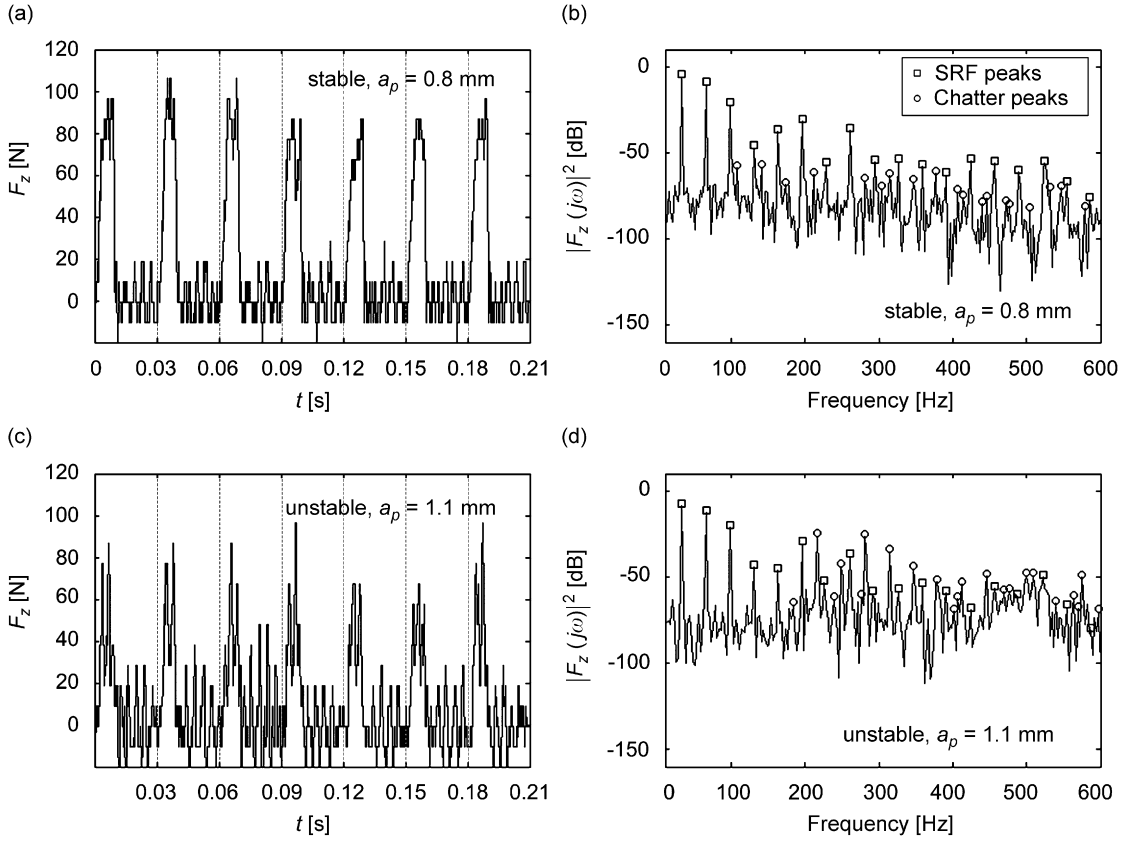

Fig. 6. Characteristics in time and spectra of the axial force F_z both in stable (a) and (b), and unstable conditions (c) and (d). Cutter configuration 1, $a_L = 30$ mm, $a_{L1} = 23$ mm, $n = 1870$ rev/min, $f_z = 0.07$ mm.

When the system is stable, the auto-correlation coefficient is approximately 1, whereas it decreases to 0 when the aperiodic component becomes dominant.

The auto correlation chatter indicator—CI_{AC} was defined as follows:

$$CI_{AC} = \sqrt{1 - \rho_S^2}. \tag{3}$$

The CI_{AC} indicator is effective when the signal to noise ratio is high.

4.2.2. Frequency-domain chatter indicators

The aperiodic component of the signal $S_a(t)$ in Eq. (1), can be further decomposed into two terms as follows:

$$S_a(t) = S_c(t) + S_n(t), \tag{4}$$

where $S_c(t)$ is the aperiodic component due to chatter and $S_n(t)$ is the aperiodic component due to environmental noise. The two components were supposed to be uncorrelated. The energy E of the signal $S(t)$ can be expressed as the sum

$$E = E_p + E_c + E_n, \tag{5}$$

where E_p is the energy of $S_p(t)$, E_c is the energy of $S_c(t)$ and E_n is the energy of $S_n(t)$.

The energy of the signal E is a function both of the machining parameters and the system vibrations. The energy E_c is negligible when the system is stable and it increases when the system becomes unstable. All these

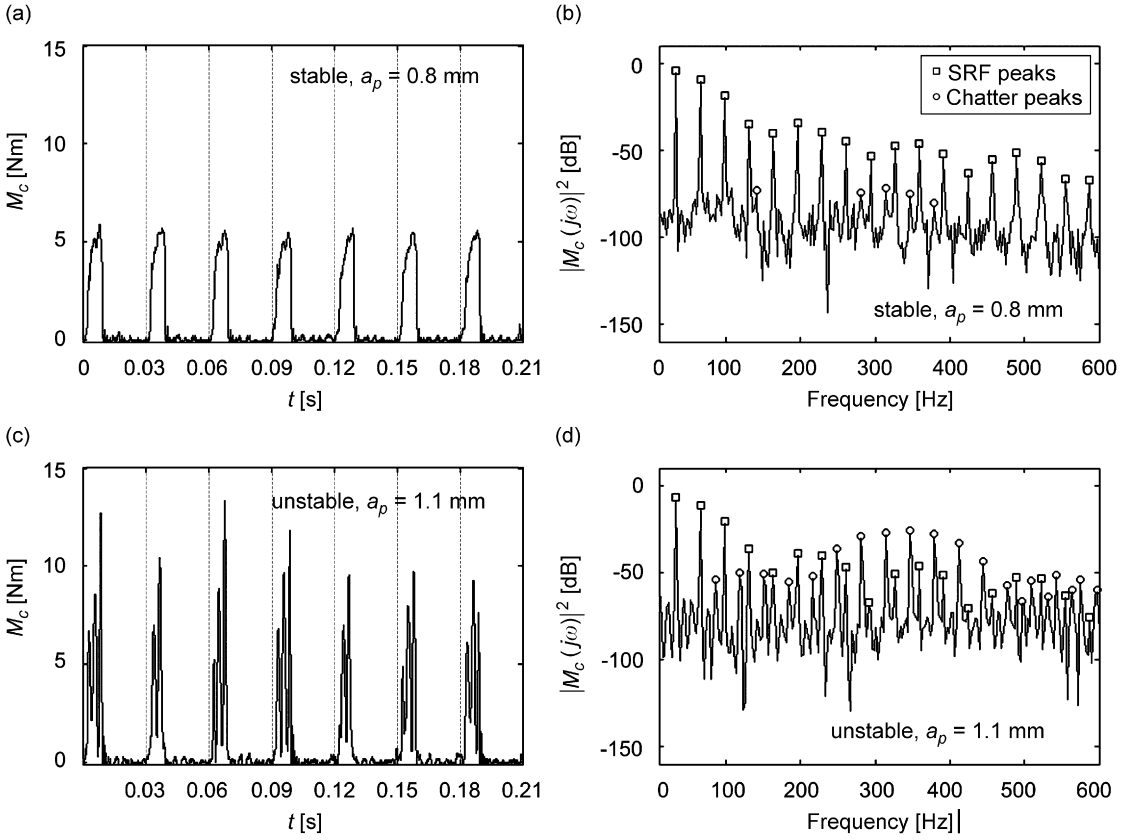

Fig. 7. Characteristics in time and spectra of the cutting torque force M_c both in stable (a) and (b), and unstable conditions (c) and (d). Cutter configuration 1, $a_L = 30\,\text{mm}$, $a_{LI} = 23\,\text{mm}$, $n = 1870\,\text{rev/min}$, $f_z = 0.07\,\text{mm}$.

energies can be estimated from power spectral density PSD_S of the signal $S(t)$, as follows:

$$E = \int_0^{+\infty} \text{PSD}_\text{S}(\omega)\,\text{d}\omega. \tag{6}$$

The energy E_p was estimated by integrating the PSD_S on small intervals of radius δ centred on the harmonics of the SRF:

$$E_p = \sum_{k=1}^{\infty}\left[\int_{k\omega_\tau-\delta}^{k\omega_\tau+\delta} \text{PSD}_\text{S}(\omega)\,\text{d}\omega,\right] \tag{7}$$

where ω_τ is the angular velocity of the spindle. The interval radius δ was set to 2 Hz after several trial and error tests.

The energy of the environmental noise component E_n was estimated by using the power spectral density PSD_0 of the signal when the cutter was rotating freely without any cutting:

$$E_n = \int_0^{+\infty} \text{PSD}_0(\omega)\,\text{d}\omega. \tag{8}$$

The energy ratio chatter indicator—CI_ER was obtained by using the ratio of energies E_c and E, as follows:

$$\text{CI}_\text{ER} = \frac{E_c}{E} = 1 - \frac{E_p + E_n}{E}. \tag{9}$$

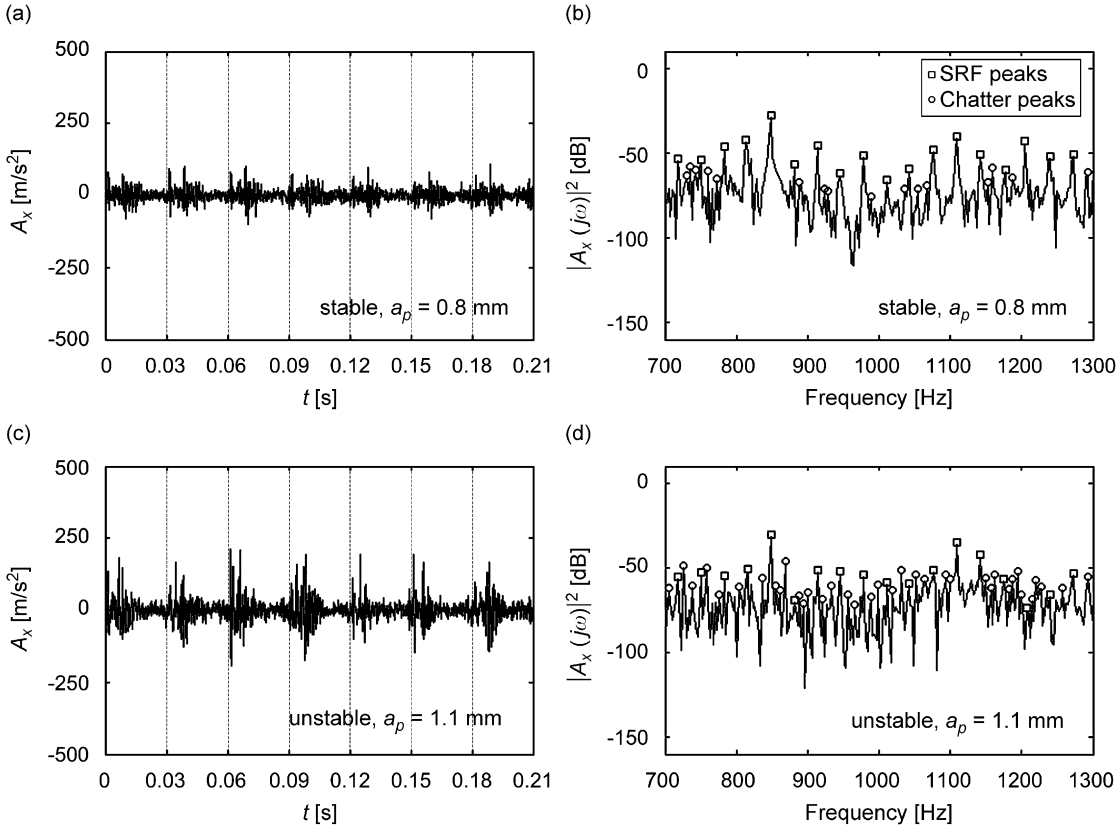

Fig. 8. Characteristics in time and spectra of the acceleration in the X direction A_X both in stable (a) and (b), and unstable conditions (c) and (d). Cutter configuration 1, $a_L = 30$ mm, $a_{L1} = 23$ mm, $n = 1870$ rpm, $f_z = 0.07$ mm.Cutter configuration 1, $a_L = 30$ mm, $a_{L1} = 23$ mm, $n = 1870$ rev/min, $f_z = 0.07$ mm.

It has to be pointed out that, for signals with low signal to noise ratio, such as A_X or A_Y, the estimation of the environmental noise energy E_n is fundamental for a successful chatter identification.

4.2.3. Time–frequency-domain chatter indicators

Wavelet packet decomposition was applied to obtain the third chatter indicator. The signal was decomposed on 6 levels by using Daubechies D8 wavelet and the signal components—approximant S_{d7} and details S_{d6}, S_{d5}, S_{d4}, S_{d3}, S_{d2} and S_{d1} signals—were calculated. For each component j, the aperiodic component of the signal $S_{dj,a}$ was calculated by subtracting from the component signal S_{dx} the periodic component $S_{dj,p}$, obtained by averaging the component signal on the basis of the spindle revolution period τ, as follows:

$$S_{dj,a}(t) = S_{dj}(t) - S_{dj,p}(t) = S_{dj}(t) - \frac{\sum_{k=1}^{N} S_{dj}(t + k\tau)}{N}; \quad j = 1, 2, 3, 4, 5, 6, 7. \tag{10}$$

The ratio of the energy of aperiodic signal to the energy of the signal r_{dj} was then determined:

$$r_{dj} = \frac{\int_0^t S_{dj,a}^2(\theta)\,\mathrm{d}\theta}{\int_0^t S_{dj}^2(\theta)\,\mathrm{d}\theta}; \quad j = 1, 2, 3, 4, 5, 6, 7. \tag{11}$$

When the system is stable, the aperiodic component is small and the energy ratio r_{dj} is ideally 0, whereas the periodic component $S_{dj,p}$ is very small and the energy ratio is close to 1 in unstable conditions.

According to the preliminary analysis, the energy ratio of the S_{d6} detail signal, r_{d6}, is a good chatter indicator for all sensors except the electrical power sensor. In general, the selection of which detail signal to

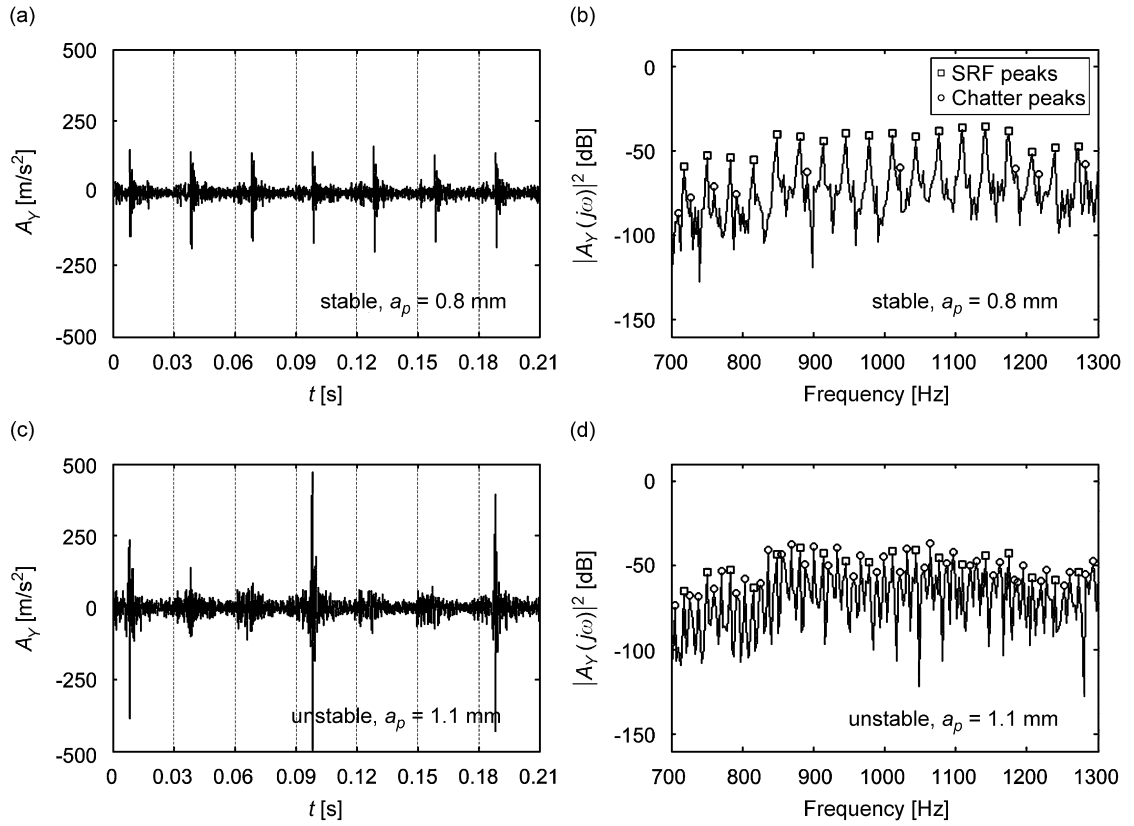

Fig. 9. Characteristics in time and spectra of the acceleration in the Y direction A_Y both in stable (a) and (b), and unstable conditions (c) and (d). Cutter configuration 1, $a_L = 30$ mm, $a_{LI} = 23$ mm, $n = 1870$ rev/min, $f_z = 0.07$ mm.

apply for chatter detection should be in accordance to the dynamical characteristics of the mechanical system. In this way, the wavelet decomposition chatter indicator—CI_{WD} was obtained.

4.3. Reference chatter indicator—CI_E

Due to their sensitivity to chatter, a combination of both indicators of the feed force F_f and feed perpendicular force F_{fN} was selected as the reference chatter indicator—CI_E, as follows:

$$CI_E = \max\{CI_{ER,F_f}, CI_{ER,F_{fN}}\}. \tag{12}$$

The value of 0.2 was chosen as the critical value CV_{CIE}, i.e. all experimental points with a CI_E value equal or greater than 0.2 were considered unstable.

Since the rotating dynamometer is not suitable for application in industrial conditions, the feed force and feed perpendicular force signals were used only as a reference in laboratory conditions and they are neglected in the following discussion.

4.4. Comparison of indicators

For each chatter indicator CI, the critical value CV was selected. The CV determines whether the chatter indicator classifies as stable, $CI < CV$, or unstable, $CI \geqslant CV$, the machining system. The four possible cases of the estimation of a generic chatter indicator against the reference chatter indicator are given in Table 4. In cases 1 and 3 the chatter indicator correctly identifies the state of the machining system. The chatter indicator

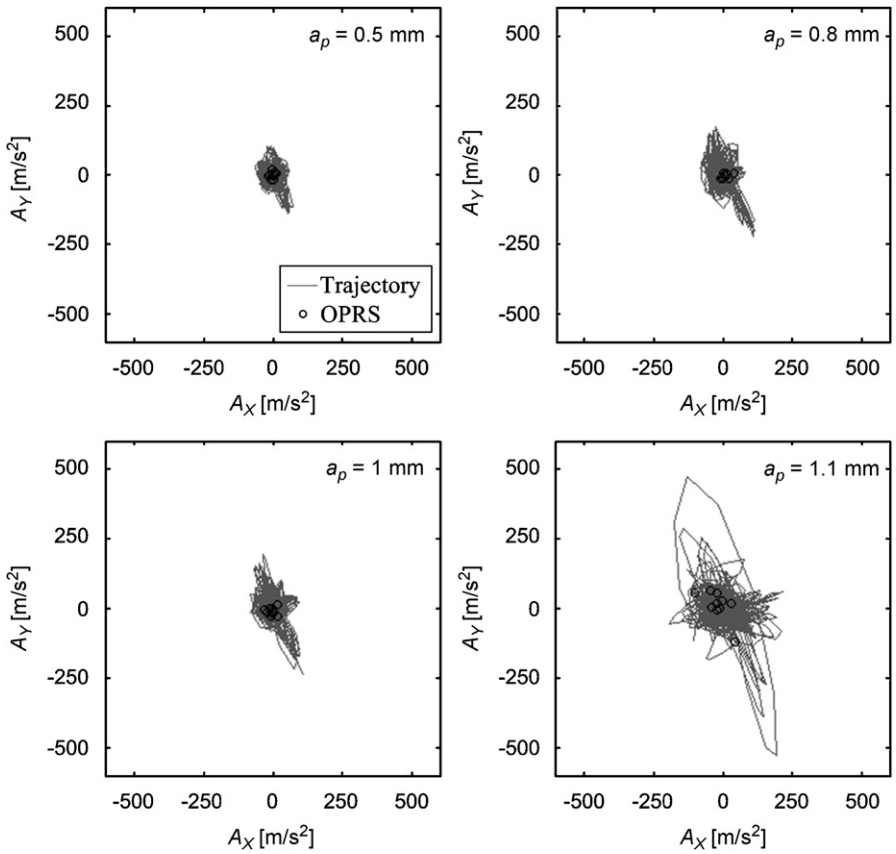

Fig. 10. Analysis of the trajectory of the system and OPRS in the A_X and A_Y plane. Cutter configuration 1, $a_L = 30$ mm, $a_{LI} = 23$ mm, $n = 1870$ rev/min, $f_z = 0.07$ mm.

fails in both cases 2 and 4. The most critical condition is case 2, where the system is unaware of the chatter onset and no countermeasures are adopted.

The critical value CV was determined automatically in order to minimize the number of stable experimental observations identified as unstable $N_{S,U}$ and number of unstable points identified as stable $N_{U,S}$.

For each chatter indicator CI, the discrete chatter indicator—DCI was defined:

$$\mathrm{DCI} = \begin{cases} 0 & \text{when} \quad \mathrm{CI} < \mathrm{CV}, \\ 1 & \text{when} \quad \mathrm{CI} \geqslant \mathrm{CV}. \end{cases} \tag{13}$$

The scatter diagrams of the sensors' indicators against the reference chatter indicator—CI_E are given in Fig. 13. The features of the different chatter indicators are summarized in Table 5.

Table 5 indicates the signal name, the name of the chatter indicator, the critical value CV, the experimental points distribution in the four cases $N_{S,S}$, $N_{U,S}$, $N_{U,U}$ and $N_{S,U}$ and the accuracy of the classification AC.

The accuracy of the classification was estimated as the percentage of experimental cases classified correctly, Eq. (14). This percentage was corrected in order to take into account the unbalance of stable and unstable experimental points. An accuracy of 50% or less would mean that the system is not able to identify the actual state of the system.

$$\mathrm{AC} = \left(0.5\frac{N_{S,S}}{N_{S,S}+N_{S,U}} + 0.5\frac{N_{U,U}}{N_{U,S}+N_{U,U}}\right)\%. \tag{14}$$

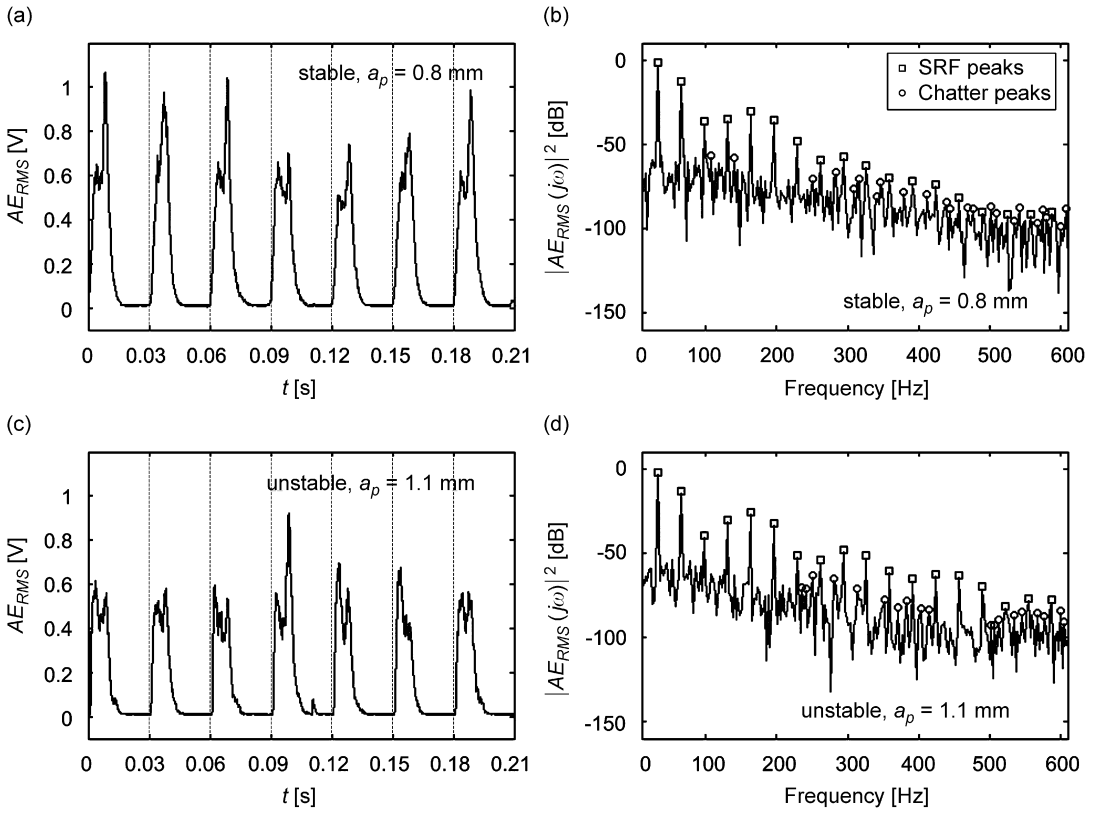

Fig. 11. Characteristics in time and spectra of the acoustic emission AE_{rms} both in stable (a) and (b), and unstable conditions (c) and (d). Cutter configuration 1, $a_L = 30$ mm, $a_{L1} = 23$ mm, $n = 1870$ rev/min, $f_z = 0.07$ mm.

The CI_{AC} of the axial force F_z and of the cutting torque M_z are good chatter indicators, whereas the CI_{AC}s of both accelerations and electrical power are poor since their signal to noise ratio is low. The CI_{AC} is the best chatter indicator among those obtained from the AE_{rms} signal.

The CI_{ER} indicator is very good for the axial force F_z, for the cutting torque M_z, and for both acceleration signals A_X and A_Y. In general, the CI_{ER} indicators are more effective than CI_{AC} indicators for chatter detection. The characteristics of the CI_{WD} indicators are comparable to those of the CI_{ER} indicators.

The CI_{ER} and CI_{WD} indicators obtained from analysis of the AE_{rms} signal are average, whereas they are very poor in the case of the P_{el} sensor.

The DCI_{AC}, DCI_{ER} and DCI_{WD} indicators were combined to obtain the combined discrete chatter indicator—DCI_C for each sensor as illustrated in Table 6.

The value of DCI_C was set to 1, when probability of the machining system being unstable given the combination of discrete chatter indicators $p(U|abc)$ was greater or equal to 0.2. This probability was obtained by analysis of the experimental data.

The reference value of 0.2 was carefully selected in order to lower the number of unstable point classified as stable. The reference value of 0.5 would have been more rigorous.

The distribution of experimental points, the conditional probabilities and the accuracy of the DCI_C for the different signals are given in Table 7, where $p(S|0)$ and $p(U|0)$ are the conditional probabilities for the system to be stable or unstable when the DCI_C is 0, respectively, and $p(S|1)$ and $p(U|1)$ are the conditional probabilities for the system to be stable or unstable when the DCI_C is 1, respectively. The Bayes theorem was applied to estimate these probabilities and the different number of stable and unstable experimental points was taken into account.

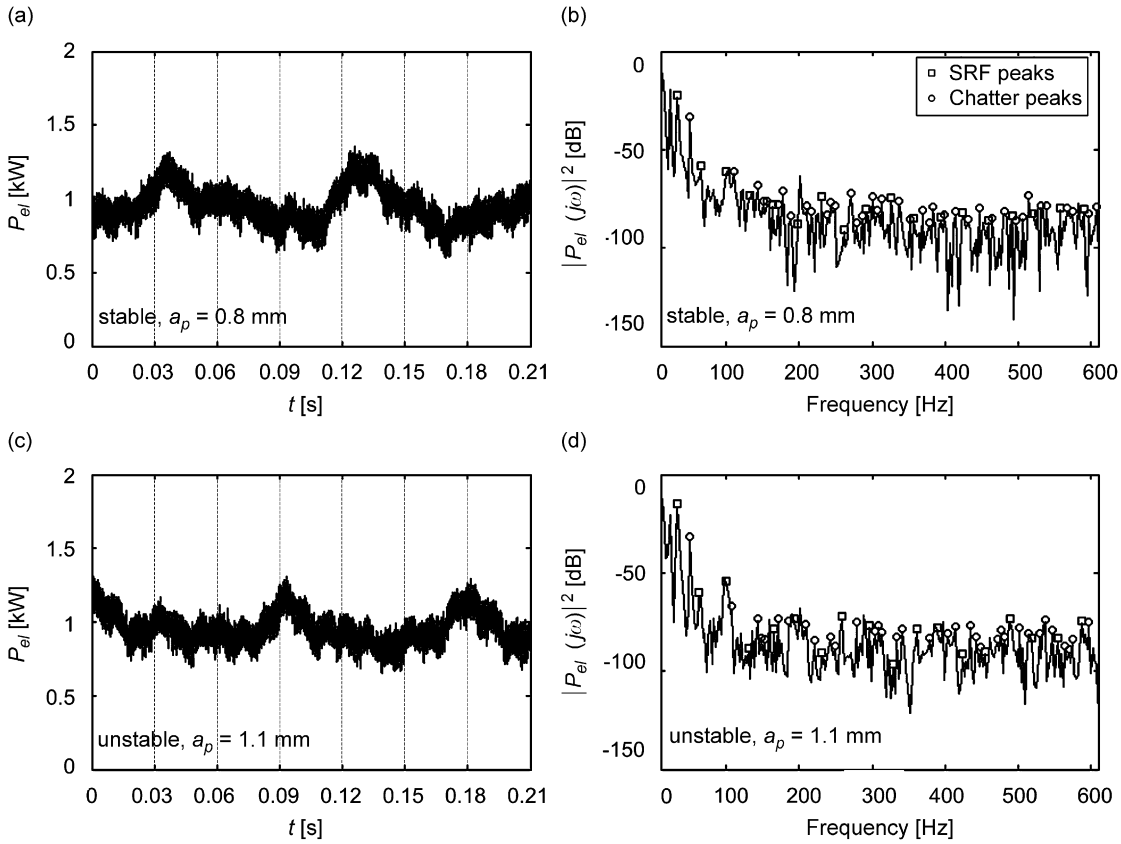

Fig. 12. Characteristics in time and spectra of the spindle power P_{el} both in stable (a) and (b), and unstable conditions (c) and (d). Cutter configuration 1, $a_L = 30$ mm, $a_{L1} = 23$ mm, $n = 1870$ rev/min, $f_z = 0.07$ mm.

Table 4
Classification cases

		Reference chatter indicator—CI_E			
		$CI_E < CV_{CIE}$		$CI_E \geqslant CV_{CIE}$	
Chatter indicator—CI	$CI \geqslant CV$	(4) System is stable and it is classified as unstable		(3) System is unstable and it is classified as unstable	
		TOLERABLE	$N_{S,U}$	CORRECT	$N_{U,U}$
	$CI < CV$	(1) System is stable and it is classified as stable		(2) System is unstable and it is classified as stable	
		CORRECT	$N_{S,S}$	MAJOR FAILURE	$N_{U,S}$

The accuracies of the DCI_C are high except in the case of the AE_{rms} and P_{el} signals. Specifically, M_z has an accuracy of 97%, and it is very effective for the identification of chatter. Indeed, the $p(S|0)$ and the $p(U|1)$ in this case are 99% and 91%, respectively. The combined discrete chatter indicators of the axial force F_z and of the acceleration signal A_Y are also very good and the DCI_C of the acceleration signal A_X is good as well.

The accuracy of DCI_C obtained from analysis of the AE_{rms} signal and of the P_{el} signal are better than those of their chatter indicators. The number of stable points classified as unstable $N_{S,U}$ of the DCI_C obtained from the AE_{rms} signal is very high. Also, the number of unstable points classified as stable $N_{U,S}$ by the DCI_C of the P_{el} signal is unacceptable.

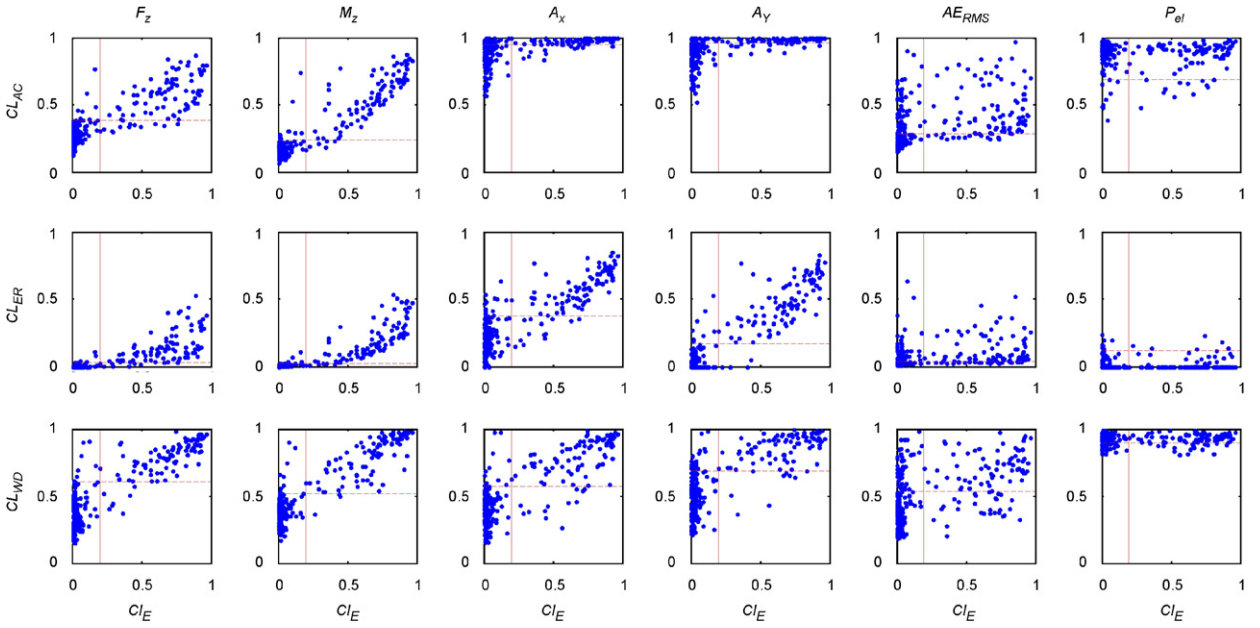

Fig. 13. Diagrams of the chatter indicators CI_{AC}, CI_{ER} and CI_{WD} against the reference chatter indicator CI_E for different sensors.

Table 5
Comparison of basic chatter indicators for different sensors

Sig.	CI	CV	$N_{S,S}$	$N_{U,S}$	$N_{U,U}$	$N_{S,U}$	AC (%)
F_z	CI_{AC}	0.39	183	12	84	8	92
	CI_{ER}	0.03	187	7	89	4	95
	CI_{WD}	0.61	182	8	88	9	93
M_z	CI_{AC}	0.24	180	6	90	11	94
	CI_{ER}	0.03	187	6	90	4	96
	CI_{WD}	0.52	183	3	93	8	96
A_X	CI_{AC}	0.95	140	15	81	51	79
	CI_{ER}	0.37	176	13	83	15	89
	CI_{WD}	0.58	179	12	84	12	91
A_Y	CI_{AC}	0.96	159	15	81	32	84
	CI_{ER}	0.17	183	4	92	8	96
	CI_{WD}	0.69	170	7	89	21	91
AE_{rms}	CI_{AC}	0.28	131	14	82	60	77
	CI_{ER}	0.04	139	20	76	52	76
	CI_{WD}	0.53	144	27	69	47	74
P_{el}	CI_{AC}	0.69	8	11	85	183	46
	CI_{ER}	0.12	180	90	6	11	50
	CI_{WD}	0.90	33	18	78	158	49

4.5. Multisensor approach

Multisensor approach was applied in order to determine whether better classification systems can be obtained by joint application of more sensors, both in terms of accuracy and of robustness against malfunctions.

Table 6
Indexes table of the combined discrete chatter indicator—DCI_C for all sensors

a	b	c	F_z		M_z		A_X		A_Y		AE_{rms}		P_{el}	
DCI_{AC}	DCI_{ER}	DCI_{WD}	$p(U\|abc)$	DCI_C	$p(U\|abc)$	DCI_C	$p(U\|abc)$	DCI_C	$p(U\|abc)$	DCI_C	$p(U\|abc)$	DCI_C	$p(U\|abc)$	DCI_C
0	0	0	0.02	0	0.00	0	0.04	0	0.00	0	0.05	0	0.45	1
0	0	1	0.40	1	0.50	1	1.00	1	0.14	0	0.50	1	0.75	1
0	1	0	0.50	1	0.50	1	0.22	1	0.44	1	0.55	1	0.62	1
0	1	1	1.00	1	1.00	1	1.00	1	1.00	1	0.00	0	0.14	0
1	0	0	0.00	0	0.00	0	0.00	0	0.00	0	0.25	1	0.18	0
1	0	1	0.00	0	0.00	0	0.33	1	0.18	0	0.57	1	0.19	0
1	1	0	0.67	1	0.43	1	0.56	1	0.50	1	0.55	1	1.00	1
1	1	1	0.99	1	1.00	1	0.95	1	1.00	1	0.62	1	0.18	0

Table 7
Distribution of experimental points, conditional probabilities and accuracy of the DCI_C for the different sensors

Signal	$N_{S,S}$	$N_{U,S}$	$N_{U,U}$	$N_{S,U}$	$p(S\|0)$	$p(U\|0)$	$p(S\|1)$	$p(U\|1)$	AC (%)
F_z	181	3	93	10	0.98	0.02	0.1	0.9	96
M_z	180	1	96	10	0.99	0.01	0.09	0.91	97
A_X	168	5	91	23	0.97	0.03	0.2	0.8	92
A_Y	183	4	92	8	0.98	0.02	0.08	0.92	96
AE_{rms}	124	7	89	67	0.95	0.05	0.43	0.57	79
P_{el}	189	89	7	2	0.68	0.32	0.22	0.78	53

Every possible combinations of sensors and signals was considered, (Tables 8 and 9). For every combination, the probability of the machining system being unstable given the combination of the DCI_Cs for the signals included in the combination was roughly estimated as follows:

$$p(U|R_1, ..., R_M) = \frac{\Pi_{k=1}^{M} p_k(U|R_k)}{\Pi_{k=1}^{M} p_k(S|R_k) + \Pi_{k=1}^{M} p_k(U|R_k)}, \tag{15}$$

where M is the number of discrete chatter indicators, $p_k(S|R_k)$ and $p_k(U|R_k)$ are the conditional probabilities of the system to be stable (S) or unstable (U), respectively, given that DCI_{Ck} is R_k (Table 7).

This approximate method was the best way to estimate the conditional probability given that the number of experimental points was not sufficient for all sensor combinations.

Like the other chatter indicators, the $p(U|R_1,\ldots,R_M)$ is defined in the range between 0 and 1. The critical value was set to 0.2.

In Table 8, the multisensor systems composed of a combination of two and three signals are illustrated, while the systems composed of four, five and six signals are given in Table 9. Both tables are organized to indicate the progressive number of the classification system, the number of sensors considered M, the sensors applied in the classification system, the experimental points distribution in the four cases $N_{S,S}$, $N_{U,S}$, $N_{U,U}$ and $N_{S,U}$, the accuracy of the classification AC and the insensitivity to malfunctions rating AC_R. The rows of both tables are sorted in ascending order of number of sensors, of accuracy AC and of insensitivity to malfunctions rating AC_R.

The insensitivity to malfunction rating AC_R represents the minimum residual accuracy when one of the sensors in the considered configuration is malfunctioning. To estimate this value, the accuracy of the classification system was tested with the actual values of one of the DCI substituted with zeros, ones or random values. This procedure was repeated for all sensors and for all configurations and the worst accuracy was taken as a reference. A value of AC_R equal or less than 50% would mean that the estimation system is not robust against malfunctions.

The classification systems based on the combination of two sensors are given in the first half of Table 8. When a combination of a good sensor and of an average sensor are considered, there is no advantage since the

Table 8
Distribution of experimental points, accuracy AC and residual accuracy AC_R of the multisensor systems composed of two and three sensors

	#	F_z	M_z	A_X	A_Y	AE_{rms}	P_{el}	$N_{S,S}$	$N_{U,S}$	$N_{U,U}$	$N_{S,U}$	AC (%)	AC_R (%)
2 sensors	1					X	X	189	89	7	2	53	50
	2			X		X		168	5	91	23	91	50
	3			X			X	168	5	91	23	91	50
	4	X		X				181	3	93	10	96	50
	5				X		X	183	4	92	8	96	50
	6	X					X	181	3	93	10	96	50
	7	X				X		181	3	93	10	96	50
	8				X	X		183	4	92	8	96	50
	9			X	X			183	4	92	8	96	50
	10		X	X				181	0	96	10	97	50
	11		X			X		181	0	96	10	97	50
	12		X				X	181	0	96	10	97	50
	13	X	X					186	3	93	5	97	50
	14	X			X			188	5	91	3	97	50
	15		X		X			188	4	92	3	97	50
3 sensors	16			X		X	X	180	11	85	11	91	50
	17	X		X		X		177	2	94	14	95	79
	18	X				X	X	181	3	93	10	96	50
	19				X	X	X	183	4	92	8	96	50
	20	X		X			X	187	6	90	4	96	50
	21			X	X		X	188	7	89	3	96	50
	22	X			X		X	187	5	91	4	96	53
	23			X	X	X		178	2	94	13	96	79
	24		X			X	X	181	0	96	10	97	50
	25		X	X			X	184	3	93	7	97	50
	26		X	X		X		182	1	95	9	97	50
	27	X			X	X		183	2	94	8	97	81
	28	X	X			X		181	0	96	10	97	82
	29	X	X	X				181	1	95	10	97	91
	30		X	X	X			183	1	95	8	97	92
	31	X	X				X	186	2	94	5	98	50
	32		X		X		X	188	3	93	3	98	50
	33		X		X	X		182	0	96	9	98	81
	34	X		X	X			186	2	94	5	98	91
	35	X	X		X			186	2	94	5	98	95

latter is ignored. For instance the characteristics of combinations number 10, 11 and 12 are the same of the M_z sensor alone. The highest values of accuracy were achieved when the cutting torque sensor was applied. Combination number 14 is quite interesting since F_z and A_Y were applied and the accuracy was slightly greater than those of the two sensors taken separately.

According to these considerations, there is no advantage in the application of two-sensor systems compared to single-sensor systems, since the accuracies are comparable to those of single-sensor systems and the residual accuracy is 50% for all configurations.

The identification systems based on three sensors have an accuracy only a just greater than that of two sensors systems and the maximum accuracy is 98%. However, the residual accuracy AC_R is in some cases significantly greater than 50%. Generally, the residual accuracy for triplets of sensors coincides with the accuracy of the worst sensor in the combination. The most interesting combinations of three sensors are number 34 and 35.

In comparison to multisensor systems based on combinations of three sensors, there is no improvement in terms of maximum accuracy when considering a system composed of four sensors, but there is a slight increase

Table 9
Distribution of experimental points, accuracy AC and residual accuracy AC_R of the multisensor systems composed of four, five and six sensors

	#	F_z	M_z	A_X	A_Y	AE_{rms}	P_{el}	$N_{S,S}$	$N_{U,S}$	$N_{U,U}$	$N_{S,U}$	AC (%)	AC_R (%)
4 sensors	36	X			X	X	X	187	5	91	4	96	52
	37	X	X	X			X	188	6	90	3	96	53
	38	X		X		X	X	187	6	90	4	96	53
	39			X	X	X	X	188	7	89	3	96	53
	40		X		X	X	X	187	3	93	4	97	52
	41	X	X		X		X	188	5	91	3	97	53
	42	X		X	X		X	188	5	91	3	97	53
	42		X	X	X		X	188	4	92	3	97	53
	44		X	X		X	X	184	3	93	7	97	53
	45	X	X	X		X		181	1	95	10	97	92
	46		X	X	X	X		183	1	95	8	97	92
	47	X	X			X	X	186	2	94	5	98	53
	48	X		X	X	X		186	2	94	5	98	92
	49	X	X	X	X			187	2	94	4	98	95
	50	X	X		X	X		186	2	94	5	98	95
5 sensors	51	X	X	X		X	X	183	1	95	8	97	53
	52	X		X	X	X	X	188	4	92	3	97	53
	53	X	X		X	X	X	186	2	94	5	98	53
	54		X	X	X	X	X	184	1	95	7	98	53
	55	X	X	X	X		X	187	2	94	4	98	95
	56	X	X	X	X	X		186	2	94	5	98	95
6 sensors	57	X	X	X	X	X	X	187	2	94	4	98	92

of the residual accuracy AC_R. Combinations number 48 and 49 are of major relevance among other four sensors combinations.

The combinations of 5 and 6 sensors are not recommended since there is no advantage neither in terms of accuracy nor residual accuracy.

5. Validation

In order to validate the approach, this methodology was applied to a new test configuration very different from those described in Section 3.

Dry milling tests were performed on an EX–CELL–O High Speed Machining center (Fig. 14).

The tooling system was composed of an HSK 63 spindle adaptor, a mechanical extension of 181 mm length and an end milling cutter. The cutter was a Stellram face milling cutter, diameter $D = 25$ mm, tool cutting edge angle $\chi = 90^\circ$, number of teeth $z = 3$, inserts ADGT12T3PDFR-721 GH1, facet. Two of the three inserts were ground in order to obtain a balanced tool with only one active tooth. Up milling tests were performed with a width of cut a_L of 6.25 mm and feed per tooth f_z of 0.1 mm.

The spindle speed was on 32 levels, from 4250 to 12,000 rev/min. In each test, the depth of cut was increased by discrete increments of 0.1 mm from 0.4 mm until severe chatter occurred. The test was stopped at a depth of cut of 1.8 mm if no chatter was observed. The total number of experimental points was 125: 99 stable points and 26 unstable points. The workpiece material was aluminium Ergal 7075, $30 \times 80 \times 250\,mm^3$, clamped directly on the plate dynamometer.

The feed force F_f, the feed perpendicular force F_{fN}, the axial cutting force F_z were measured by using a Kistler 9255B plate dynamometer. Accelerations in the X, Y and Z directions A_X, A_Y and A_Z were detected by a Kistler triaxial accelerometer type 8792A50 mounted on the spindle housing. All sensor signals were sampled at a frequency of 20 kHz by using a National Instruments data acquisition system.

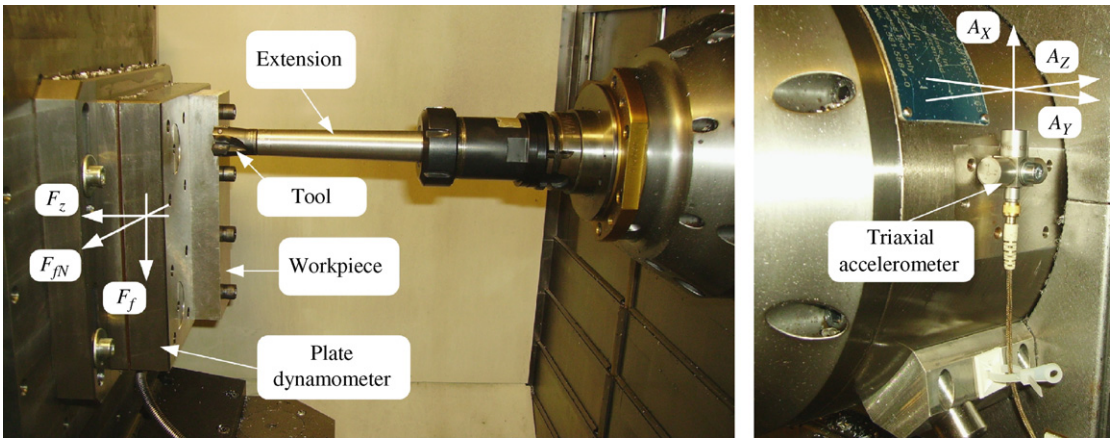

Fig. 14. Test configuration for validation of the approach.

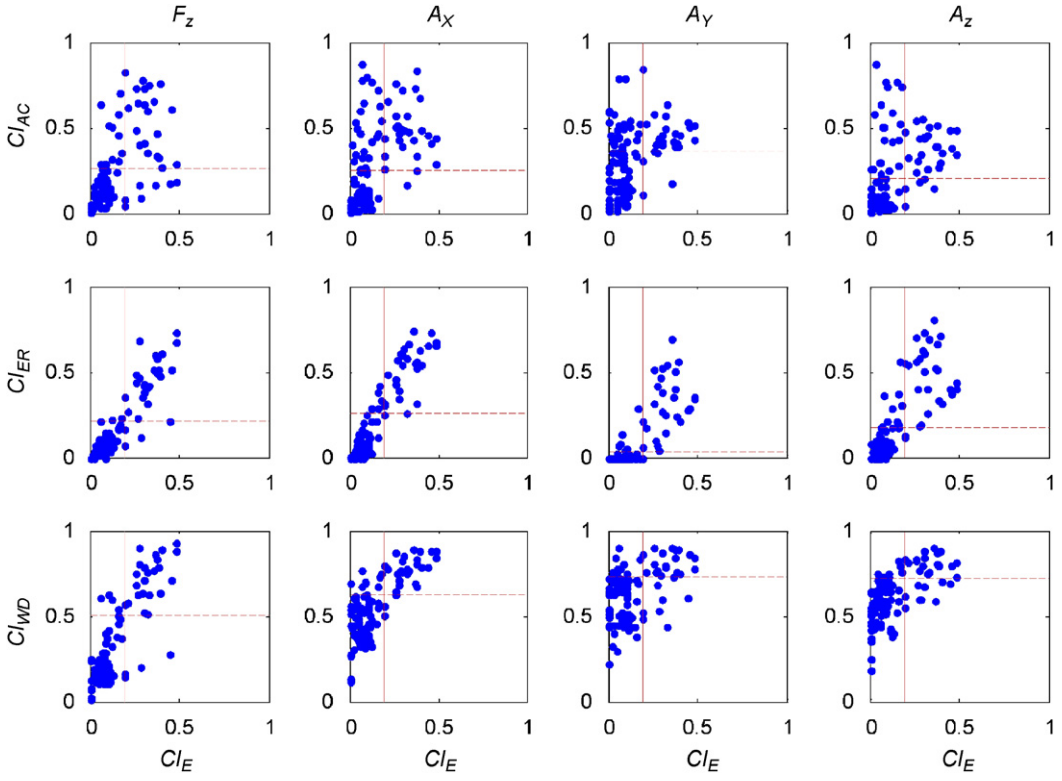

Fig. 15. Diagrams of the chatter indicators CI_{AC}, CI_{ER} and CI_{WD} against the reference chatter indicator CI_E for different sensors for the validation configuration.

The frequency response of the machining and monitoring system were estimated by applying the pulse test method. The main resonance peaks were located in the range between 500 and 1500 Hz for both cutting force and acceleration signals.

Chatter indicators were calculated according to the procedure outlined in Section 4.2. Again, the reference chatter indicator CI_E, as defined in Eq. (12), was calculated from the F_f and F_{fN} signals. In this case, the detail signal d_4 was chosen to determine the wavelet decomposition chatter indicator—CI_{WD}.

In Fig. 15, the scatter diagrams of the sensors' indicators against the reference chatter indicator—CI_E for the validation configuration are shown.

The diagrams of the chatter indicators confirmed the applicability of the approach to the new experimental set-up. Specifically, the accuracy of the DCI_C is greater than 95% for signals A_X, A_Y, and F_z, whereas it is 93% for A_Z.

Also, the multisensor approach classification system gave very good results. For instance, the classification system based on the signals F_z, A_X and A_Y is characterized by an accuracy AC of 97% and by an insensitivity to malfunctions rating AC_R of 95%.

6. Conclusions

According to the considerations presented in this work, it is possible to draw the following conclusions:

Regenerative chatter has a strong influence on the cutting force signals measured by a rotating dynamometer in face milling, and it produces variations on the signals features both in time domain and in frequency domain. The characteristic of the signals measured by accelerometers mounted on the spindle housing of the machine tool are influenced by regenerative chatter even if their sensitivity is greatly influenced by the placement of transducers.

It is not easy to determine the influences of the chatter on the acoustic emission root mean square signal and on the main spindle electrical power signal.

The rotating dynamometer can be effectively applied in face milling for chatter identification in laboratory testing by using the force components both in the feed direction and in the direction perpendicular to the feed, however its applicability in industrial conditions is limited. The axial force and the cutting torque are promising for industrial application.

The chatter indicators obtained from the analysis of the axial cutting force F_z, the cutting torque M_z and the accelerations can be applied for chatter detection in face milling. Specifically, the indicators derived from the cutting torque M_z are more reliable than other indicators.

The chatter identification is less reliable, when only the acoustic emission AE_{rms} signal is applied. It is not useful to apply the chatter indicators obtained from the electrical power P_{el} sensor.

The multisensor combinations of three or four sensors are strongly recommended, since it is possible to achieve high levels of accuracy and of robustness against malfunctions. For example, the multisensor system composed of the axial force sensor and accelerometers A_X and A_Y is a very promising solution for reliable and robust chatter identification.

The validation confirmed the applicability of the approach to experimental conditions very different from those where it was first developed and tested.

It would be of further interest to apply the obtained results in new machining systems.

References

[1] J. Gradisek, M. Kalveram, T. Insperger, K. Weinert, G. Stépán, E. Govekar, I. Grabec, On stability prediction for milling, *International Journal of Machine Tools and Manufacture* 45 (2005) 768–781.

[2] Y. Altintas, M. Weck, Chatter stability of metal cutting and grinding, *Annals of the CIRP* 53/2 (2004) 619–642.

[3] M. Weck, E. Verhaag, M. Gathier, Adaptive control for face milling operations with strategies for avoiding chatter vibrations and automatic cut distribution, *Annals of the CIRP* 24/1 (1975) 405–409.

[4] S.Y. Liao, Y.C. Young, A new on-line spindle speed regulation strategy for chatter control, *International Journal of Machine Tools and Manufacture* 36/5 (1996) 651–660.

[5] Y.S. Tarng, E.C. Lee, A critical investigation of the phase shift between the inner and the outer modulation for the control of machine tool chatter, *International Journal of Machine Tools and Manufacture* 37/12 (1997) 1661–1672.

[6] Y. S. Tarng, Use of Various Signals for Milling Cutter Breakage Detection, PhD Thesis, University of Florida, Gainesville, USA, 1988.

[7] T. Delio, J. Tlusty, S. Smith, Use of audio signals for chatter detection and control, *ASME Journal Engineering for Industry* 114 (1992) 146–157.

[8] X.Q. Li, Y.S. Wong, A.Y.C. Nee, Tool wear and chatter detection using the coherence function of two crossed accelerations, *International Journal of Machine Tools and Manufacture* 37/4 (1996) 425–435.

[9] M. Hashimoto, E. Marui, S. Kato, Experimental research on cutting force variation during regenerative chatter vibration in a plain milling operation, *International Journal of Machine Tools and Manufacture* 36 (1996) 1073–1092.
[10] O. Ryabov, K. Mori, N. Kasashima, Laser displacement meter application for milling diagnostics, *Optics and Lasers in Engineering* 30 (1998) 251–263.
[11] J. Gradisek, E. Govekar, I. Grabec, Using coarse-grained entropy rate to detect chatter in cutting, *Journal of Sound and Vibration* 214/5 (1998) 941–952.
[12] J. Gradisek, E. Govekar, I. Grabec, Time series analysis in metal cutting: chatter versus chatter free cutting, *Mechanical System and Signal Processing* 12/6 (1998) 839–854.
[13] T.L. Schmitz, M.A. Davies, K. Medicus, J. Snyder, Improving high-speed machining material removal rates by rapid dynamic analysis, *Annals of the CIRP* 50 (2001) 263–268.
[14] C.S. Suh, P.P. Khurjekar, B. Yang, Characterisation and identification of dynamic instability in milling operation, *Mechanical Systems and Signal Processing* 16/5 (2002) 853–872.
[15] B.P. Mann, T. Insperger, P.V. Bayly, G. Stépán, Stability of up and down milling, part 2: experimental verification, *International Journal of Machine Tools and Manufacture* 43 (2003) 35–40.
[16] R.P.H. Faassen, N. van de Wouw, J.A.J. Oosterling, H. Nijmeijer, Prediction of regenerative chatter by modelling and analysis of high-speed milling, *International Journal of Machine Tools and Manufacture* 43 (2003) 1437–1446.
[17] C.K. Toh, Vibration analysis in high speed rough and finish milling hardened steel, *Journal of Sound and Vibration* 278 (2004) 101–115.
[18] W.L. Weingaertner, R.B. Schroeter, M.L. Polli, J. de Oliveira Gomesc, Evaluation of high-speed end-milling dynamic stability through audio signal measurements, *Journal of Materials Processing Technology* 179 (2006) 133–138.
[19] M. Sortino, Study on Cutting Forces and Tool Condition Monitoring in Face Milling, PhD Thesis, University of Udine, Udine, Italy, 2003.
[20] T. Insperger, G. Stépán, P.V. Bayly, B.P. Mann, Multiple chatter frequencies in milling processes, *Journal of Sound and Vibration* 262 (2003) 333–345.
[21] S.S. Park, Y. Altintas, Dynamic compensation of spindle integrated force sensors with Kalman filter, *ASME Journal of Dynamic Systems, Measurement and Control* 126 (2004) 443–452.